YMTHE, Volume *29*

Supplemental Information

METTL3 restrains papillary thyroid cancer progression via m^{6}A/c-Rel/IL-8-mediated neutrophil infiltration

Jing He, Mingxia Zhou, Jie Yin, Junhu Wan, Jie Chu, Jinlin Jia, Jinxiu Sheng, Chang Wang, Huiqing Yin, and Fucheng He

Supplemental Information

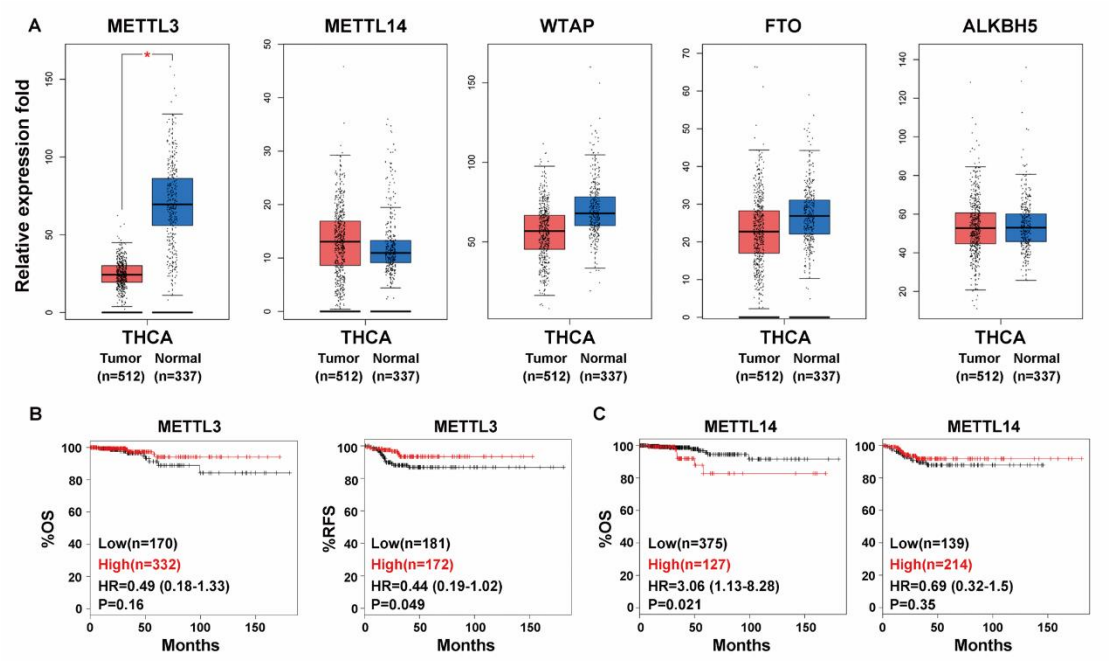

Figure S1. Decreased METTL3 expression correlates with poor prognosis of PTC patients.

(A) Expression profiles of METTL3, METTL14, WTAP, FTO and ALKBH5 mRNA level in primary PTC tissues and normal thyroid tissues from the GEPIA database. (B) and (C) Kaplan-Meier survival curves of overall survival (OS) and recurrent-free survival (RFS) of METTL3 and METTL14 in PTC patients from the Kaplan-Meier Plotter database. (*$P < 0.05$)

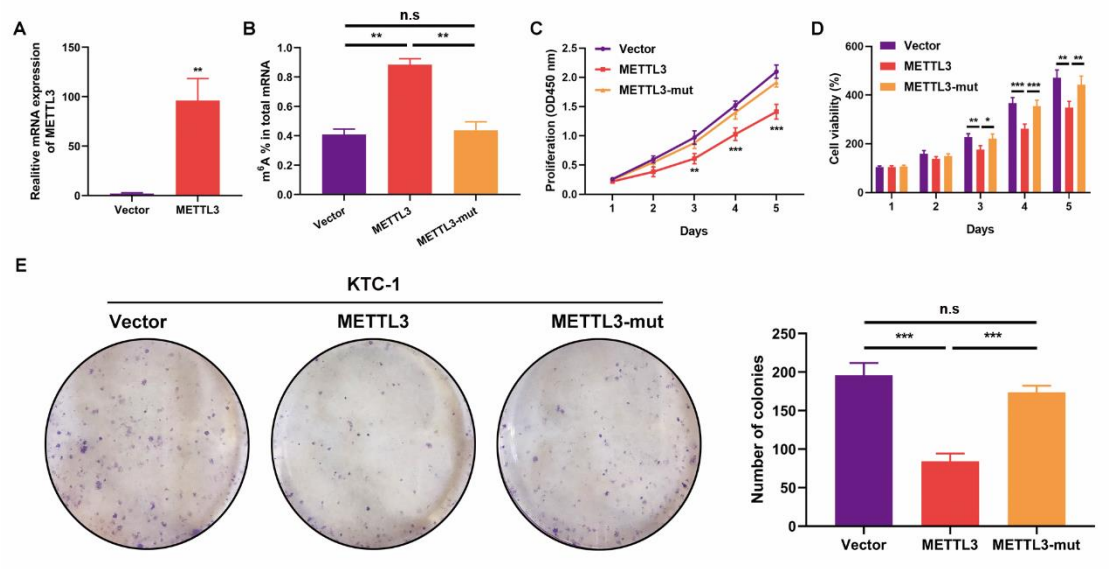

Figure S2. METTL3 mediated m^{6}A methylation inhibits PTC cells proliferation.

(A) RT-PCR analysis confirming forced overexpression of METTL3 in KTC-1 cells. (B) The m^{6}A contents of total RNAs in METTL3-overexpression and catalytic mutant METTL3 KTC-1 cells. (C) and (D) The cellular growth was analyzed by CCK8 and CellTiter-Glo Luminescence assays in KTC-1 cells transfected with METTL3 or mutant METTL3. (E) Ectopic expression of METTL3 impaired colony-formation abilities of KTC-1 cells**.** Quantification of the colony formation assay results was shown in the right panel. (*$P < 0.05$, **$P < 0.01$, ***$P < 0.001$, n.s: not significant)

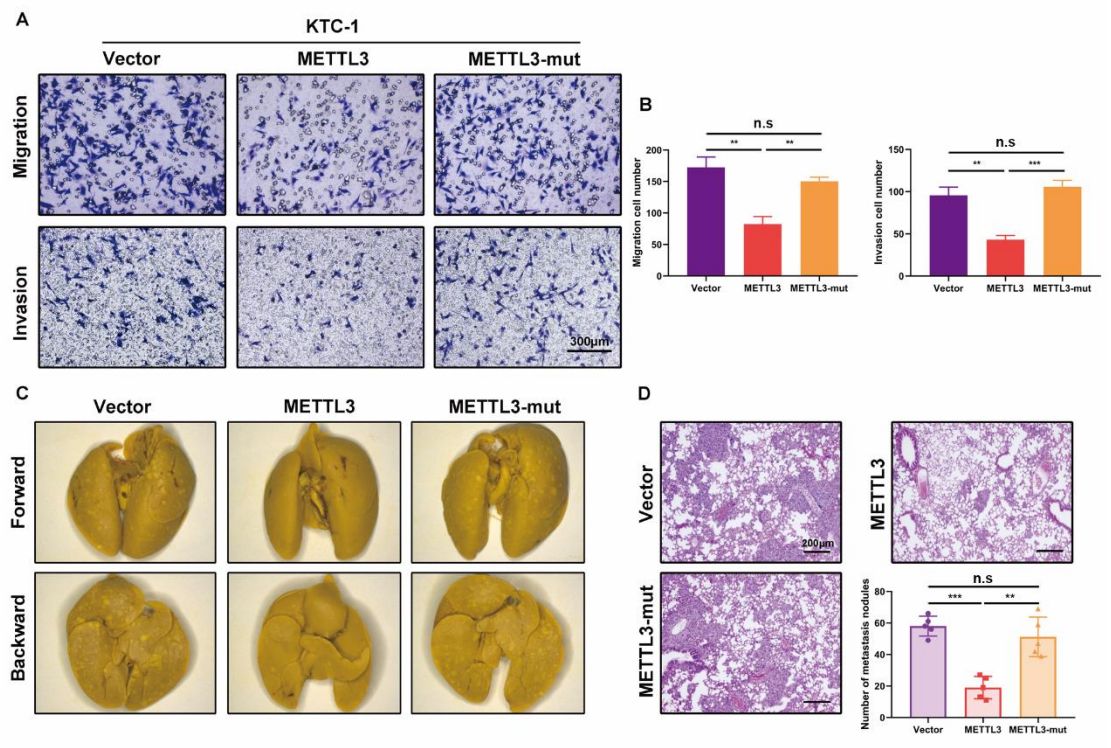

Figure S3. Enforced Expression of METTL3 suppresses the metastasis of PTC cells.

(A) The migration and invasive abilities were explored by transwell assays in KTC-1 cells with indicated plasmids. Magnification: × 200. Scale bar: 300 μm. (B) Statistical analysis of the number of migrated and invasive cells from three independent experiments. (C) KTC-1 cells stably expressing control vector, wild-type METTL3 and mutant-METTL3 were delivered into the Balb/c nude mice by tail vein injection. Representative images of lungs were harvested at the endpoint and shown (n=5 per group). (D) Representative H&E staining images and quantification of metastatic lung nodules from the indicated group of mice. Magnification: × 50. Scale bar: 200 μm. (**$P < 0.01$, ***$P < 0.001$, n.s: not significant)

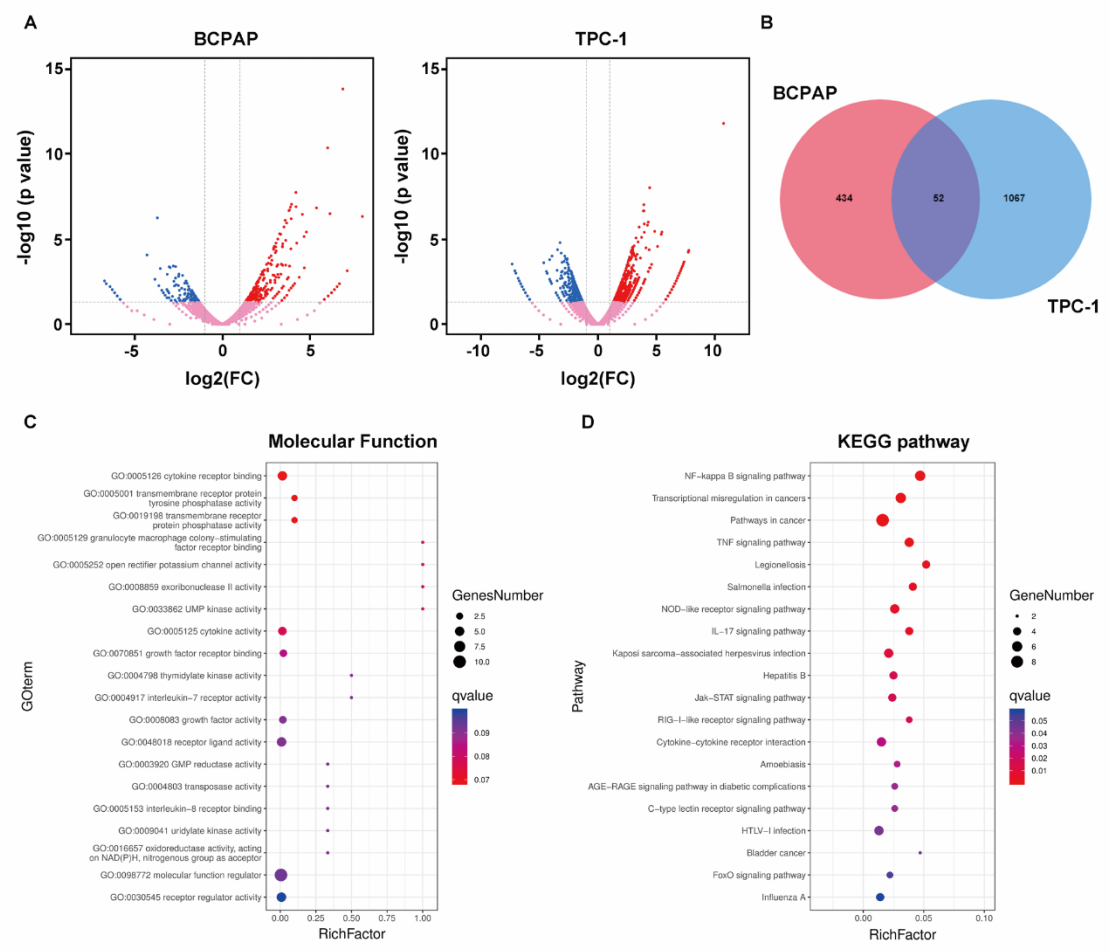

Figure S4. Identification for potential mechanisms in METTL3-involved PTC progression.

(A) Volcano plot illustrated differentially expressed genes between METTL3-knockdown relative to control BCPAP and TPC-1 cells based on RNA-seq data. | Log2FC | >1 and adjusted *P* value < 0.05 were set as cutoff criteria. (B) Venn diagram identified 52 differentially expressed genes overlap in METTL3-knockdown BCPAP and TPC-1 cells when compared to the control group. (C) and (D) Gene Ontology (GO) and KEGG enrichment analysis were performed based on 52 common differentially expressed genes in both BCPAP and TPC-1 cells.

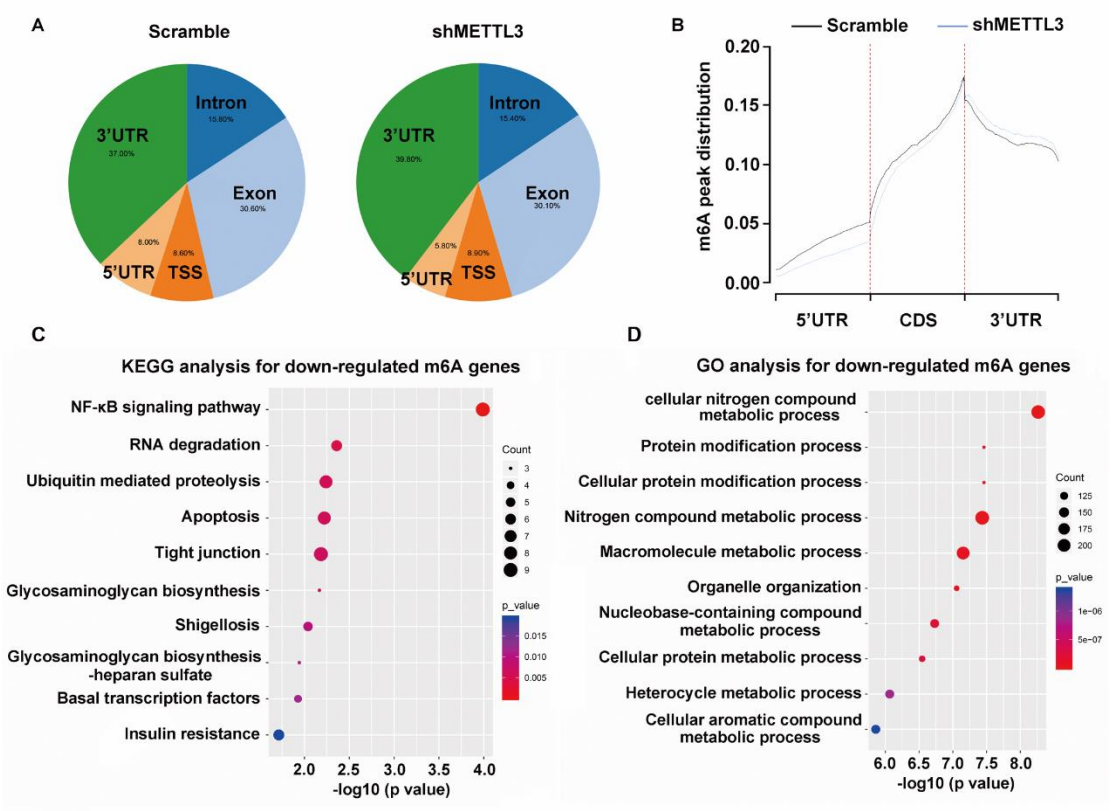

Figure S5. Bioinformatics analyses for m^{6}A-regulated genes in BCPAP cells.

(A) Proportion of m^{6}A peak distributions in the 5'UTR, TSS (transcriptional start site), exon, intron and 3'UTR region across the entire set of mRNA transcripts of control group and shMETTL3 group in BCPAP cells. (B) Density distribution of m^{6}A peaks across 5'UTR, CDS and 3'UTR mRNA transcripts in METTL3-knockdown BCPAP cells related to the control cells. (C) and (D) KEGG enrichment analysis and GO biological process of the transcripts with decreased m^{6}A methylation in BCPAP cells. Fold-change < -1.5 and adjusted *P* value < 0.05 were set as cutoff criteria.

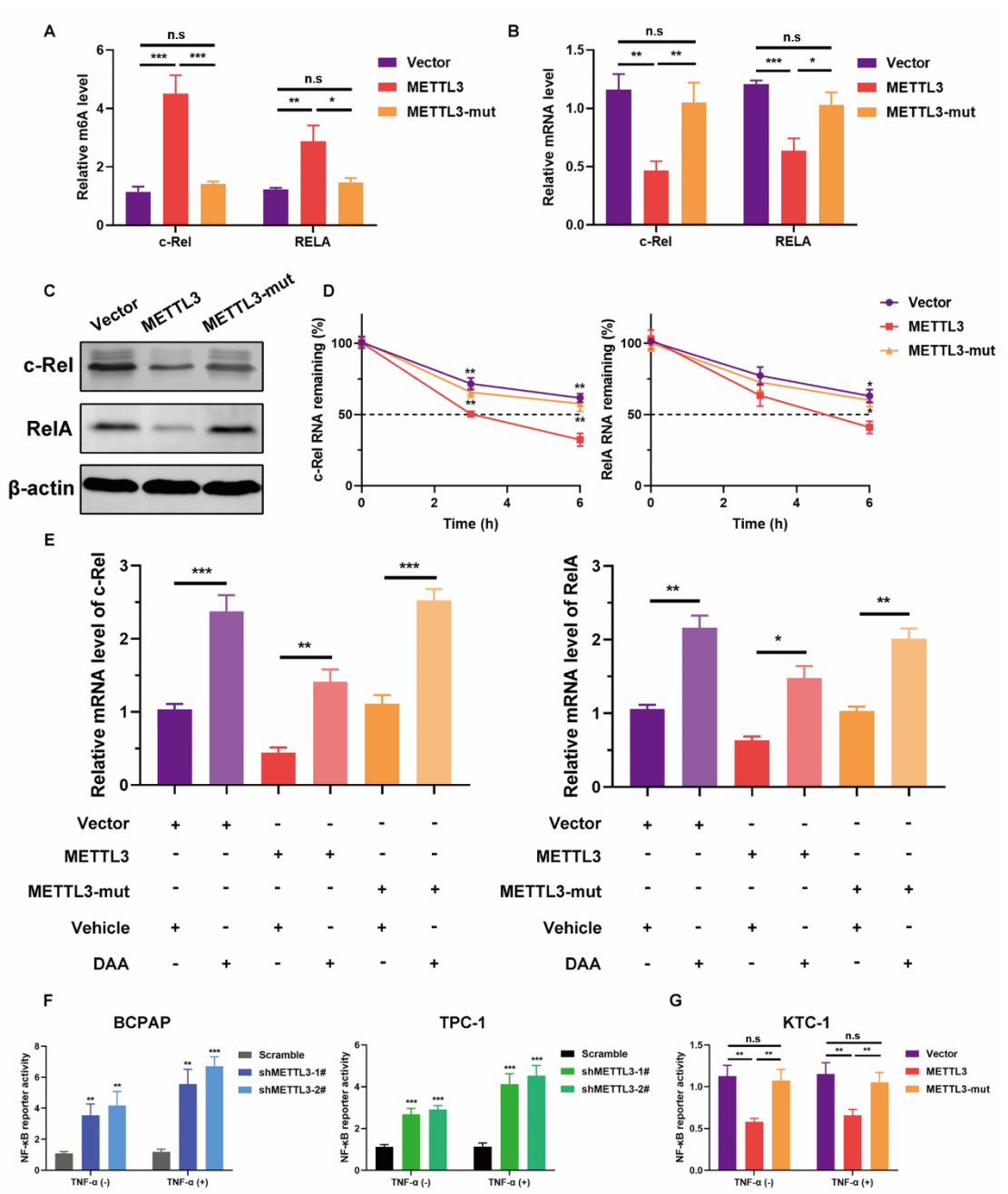

Figure S6. METTL3 regulates c-Rel and RelA mRNA stability via an m^{6}A-dependent manner.
(A) and (B) Gene-specific m^{6}A qPCR and RT-PCR analysis of alterations in the m^{6}A level (A) and mRNA level (B) of c-Rel and RelA in wild type or mutant METTL3-overexpression and control KTC-1 cells. (C) Western blot analysis of c-Rel and RelA protein levels in stable wild-type METTL3, mutant-METTL3 and control KTC-1 cells. (D) c-Rel and RelA transcript were measured at indicated time points post actinomycin D treatment in KTC-1 cells. (E) RT-PCR analysis of expression levels of c-Rel (left panel) and RelA (right panel) in KTC-1 cells transfected with indicated plasmids in the presence or absence of global methylation inhibitor DAA for 24h. (F) and (G) The activity of NF-κB pathway was measured after the transfection with NF-kB reporter plasmid vectors and Renilla luciferase vector in indicated BCPAP, TPC-1 and KTC-1 in the presence or absence of TNF-α (10 ng/mL) for 24 h. (*P < 0.05, **P < 0.01, ***P < 0.001, n.s: not significant)

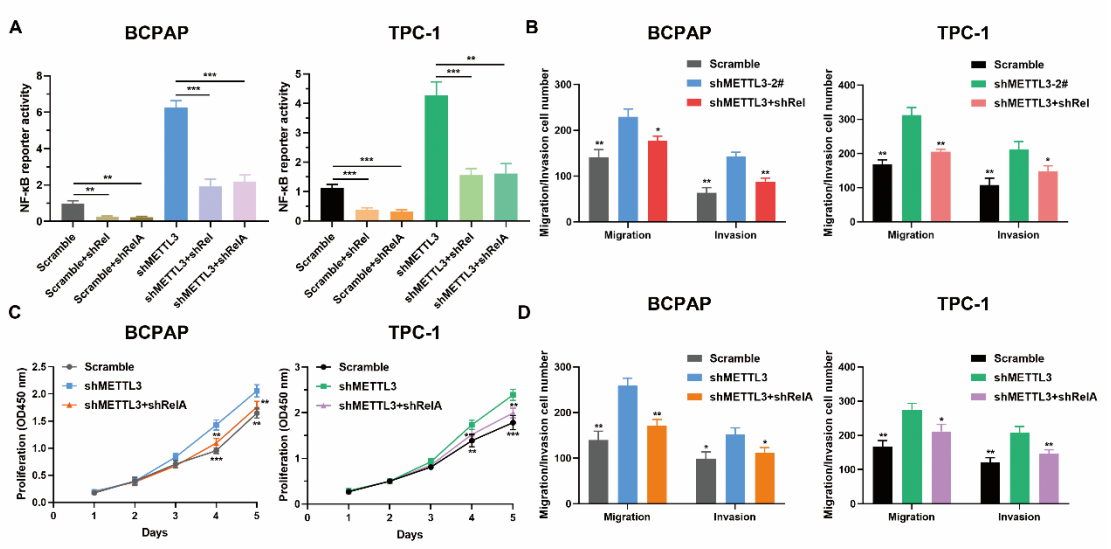

Figure S7. Depletion of c-Rel or RelA impairs METTL3-mediated malignant phenotypes of PTC cells.

(A) Relative NF-kB luciferase activity in the indicated cells with knockdown of c-Rel or RelA under the stimulation of TNF-α for 24 h. (B) Transwell migration and invasion assays were used to investigate the effects of inhibition of c-Rel on cells metastasis of METTL3-silencing BCPAP and TPC-1 cells. (C) CCK-8 assay showing that the knockdown of RelA partially rescued the proliferation inhibition of BCPAP and TPC-1 cells with the knockdown of METTL3. (D) Inhibition of RelA partially reversed the suppression of METTL3 knockdown on PTC cells migration and invasion. (*$P < 0.05$, **$P < 0.01$, ***$P < 0.001$)

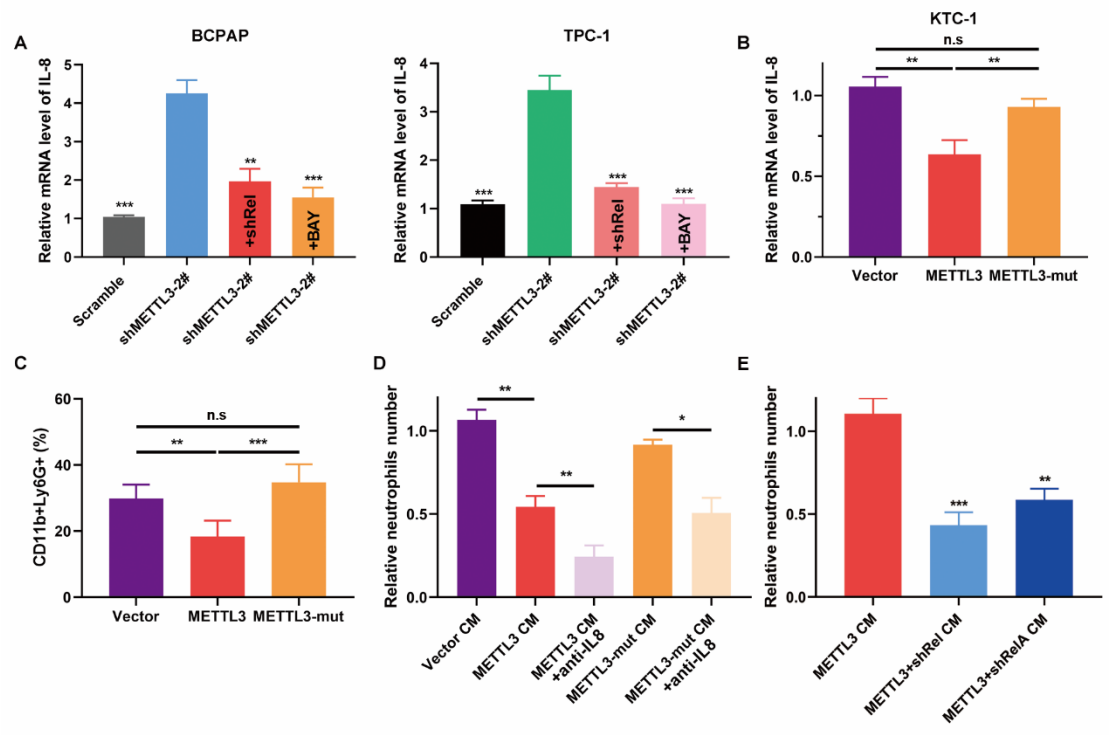

Figure S8. METTL3 regulates TANs recruitment through IL-8.

(A) IL-8 expression was inhibited in METTL3-silencing BCPAP and TPC-1 cells treated with BAY 11-7082 or knockdown of c-Rel compared to control cells. (B) Overexpression of METTL3 decreased the mRNA level of IL-8 in KTC-1 cells. (C) Flow cytometry showed inhibition of TANs ($CD45^+CD11b^+Ly6G^+$) accumulation by METTL3 overexpression in KTC-1 subcutaneous tumor tissues (n=5 mice per group). (D) Chemotaxis assay results showed that overexpression of METTL3 combined with IL-8 neutralizing antibody impedes TANs recruitment. (E) The effects of c-Rel and RelA in METTL3-mediated neutrophils recruitment. (*$P < 0.05$, **$P < 0.01$, ***$P < 0.001$, n.s: not significant)

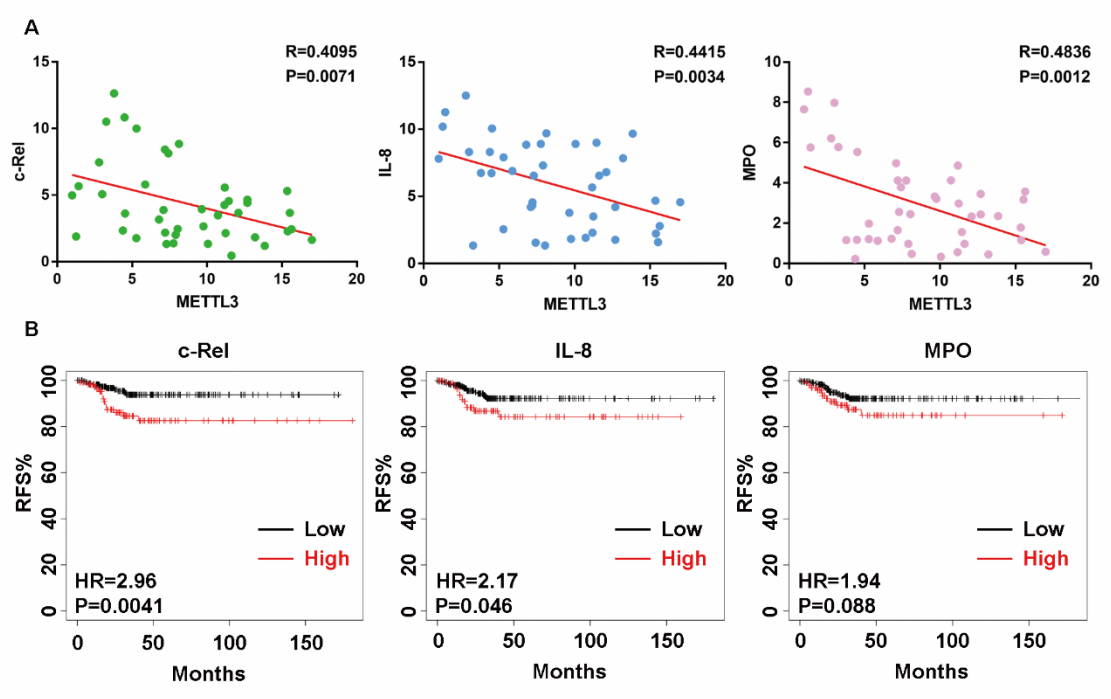

Figure S9. Clinical correlation of METTL3 and its downstream targets in PTC tissues.

(A) RT-PCR analysis of METLL3 expression and the level of c-Rel, IL-8 and MPO in PTC tissues and the corresponding correlations were presented. (B) Kaplan–Meier survival analysis of recurrent-free survival (RFS) in PTC patients with high and low level of c-Rel, IL-8 and MPO.

Table S1. The primers used in this study for RT-PCR analysis.

Genes	Forward primer (5'-3')	Reverse primer (5'-3')
METTL3	AAGCTGCACTTCAGACGAAT	GGAATCACCTCCGACACTC
METTL14	AGAAACTTGCAGGGCTTCCT	TCTTCTTCATATGGCAAATTTTCTT
WTAP	GGCGAAGTGTCGAATGCT	CCAACTGCTGGCGTGTCT
FTO	TGGGTTCATCCTACAACGG	CCTCTTCAGGGCCTTCAC
ALKBH5	CCCGAGGGCTTCGTCAACA	CGACACCCGAATAGGCTTGA
c-Rel	GCAGAGGGGAATGCGTTTTAG	AGAAGGGTATGTTCGGTTGTTG
RelA	CCCACGAGCTTGTAGGAAAGG	GGATTCCCAGGTTCTGGAAAC
IL-8	ACTGAGAGTGATTGAGAGTGGAC	AACCCTCTGCACCCAGTTTTC
MPO	CCAGATCATCACTTACCGGGA	CACTGAGTCATTGTAGGAACGG
β-actin	GCACAGAGCCTCGCCTT	CCTTGCACATGCCGGAG